九州大学学術情報リポジトリ Kyushu University Institutional Repository

Trigonal Fe_2Si Nanosheets at Fe/Amorphous SiO x Interfaces for Spintronic Nanodevices

Sato, Kazuhisa Research Center for Ultra-High Voltage Electron Microscopy, Osaka University

Fujii, Yuta Research Center for Ultra-High Voltage Electron Microscopy, Osaka University

https://hdl.handle.net/2324/7393024

出版情報: ACS Applied Nano Materials. 7 (14), pp.16799-16805, 2024-07-13. American Chemical Society (ACS)

バージョン:

権利関係: This document is the Accepted Manuscript version of a Published Work that appeared in final form in ACS Applied Nano Materials, copyright © 2024 American Chemical Society after peer review and technical editing by the publisher. To access the final edited and published work see https://doi.org/10.1021/acsanm.4c02874.



Kazuhisa Sato* and Yuta Fujii

Research Center for Ultra-High Voltage Electron Microscopy, Osaka University

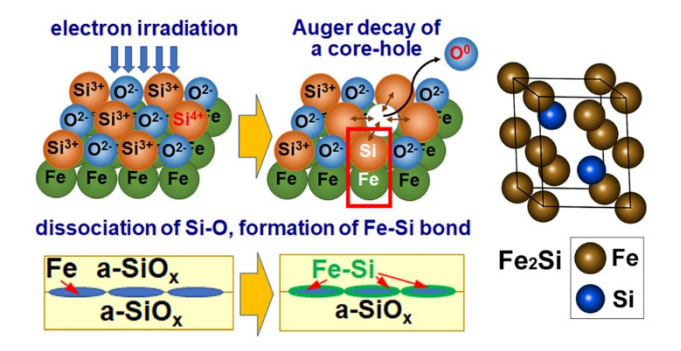
7-1 Mihogaoka, Ibaraki, 567-0047 Osaka, Japan

^{*}Corresponding author. sato@uhvem.osaka-u.ac.jp

ABSTRACT:

Trigonal Fe₂Si nanosheets, which are promising candidates for spintronics nanodevices, were synthesized at the Fe/amorphous (a-)SiO_x thin film interface using electron irradiation. The formation of nanoscale silicide was confirmed at 90 K as well as at 298 K. Such a low temperature synthesis of Fe₂Si can be attributed to the dissociation of a-SiO_x induced by electronic excitation; Si-O bonds dissociate through Auger decay of core-holes generated by electronic excitation, and then dissociated Si atoms form Fe-Si bonds. The amount of Fe₂Si formed at room temperature was greater than that at 90 K, suggesting that the atomic migration induced by electronic excitation involves contribution of thermal energy. The amount of Fe₂Si nanosheets produced indicates that the Si-O bonds are more easily dissociated by electronic excitation in a-SiO_x rather than in a-SiO₂. Formation of the Fe₂Si nanosheets found in this study differs from the formation of equiatomic FeSi phase predicted by thermodynamical models assuming diffusion at a planar Fe/Si interface. We propose a versatile route to selectively form metal silicide nanosheets in an electron irradiated area at temperatures below room temperature.

KEYWORDS: nonradiative transition, electronic excitation, Fe₂Si, nanosheets, Auger decay



INTRODUCTION

Electronic excitation triggered by electron irradiation relaxes in a short time (~10 fs) with emission of Auger electrons or characteristic x-ray, but in some cases, it may dissociate chemical bonds and hence leads to structural modification of materials¹. For example, desorption of positive oxygen ions occurs from the free surface of transition metal oxides via Knotek-Feibelman model². Such an oxygen desorption leads to dissociation of oxides. When amorphous silicon oxide (a-SiO_x) decomposes, dissociation products are chemically highly active. Recent studies revealed that an intermetallic compound, nanoscale α-Pt₂Si, is formed at the Pt/a-SiO_x (x \sim 1.5) thin film interface by electron or photon irradiation^{3, 4}. Decomposition of a-SiO_x via core-hole Auger decay is responsible for the above mentioned Pt₂Si formation. It is noted that Pt is resistive to oxidation since oxygen absorbs on the Pt surface by chemisorption⁵. We have clarified that when the Si-O bond dissociates, Si reacts with adjacent Pt, and then the composition of a-SiO_x that has released Si approaches to a-SiO₂ ⁴. Such a solid-state reaction induced by electronic excitation occurs at or even below room temperature within a selected area where electrons are irradiated⁶. The process largely differs from typical silicide formation, which involves high temperature processes. Therefore, the phenomenon has a potential application to a novel processing for a nanoscale silicide formation, including micropatterning by site-selected solid-state reaction.

Fe-Si system forms various silicides that have different stoichiometric compositions such as Fe₃Si, Fe₂Si, FeSi, and FeSi₂⁷. Among these compounds, β-FeSi₂ has attracted much interest for thermoelectric materials or light emitting materials in the infrared region, while the formation temperature is higher than 1000 K ⁸⁻¹⁰. On the other hand, trigonal Fe₂Si, a ferromagnetic half metal with 100% spin-polarization ratio, is expected as a novel spintronics material, based on electronic structure calculations, while there are few reports on this topic^{11, 12}. The advantage of Fe-Si system is that both Fe and Si are abundant resources in addition to excellent functionality that vary depending on their chemical composition.

However, synthesis of iron silicides generally requires high-temperature processes, and hence, low temperature synthesis of nanoscale silicides via the above-mentioned nonradiative transition is of technologically interest. Diffusion mechanism of atoms is also an issue that requires elucidation to understand the solid-state reaction.

In this study, we aim to form iron silicide nanosheets at the Fe/a-SiO_x thin film interface by electron irradiation and elucidate its microstructure and formation mechanism. Transmission electron microscopy (TEM) is the suitable methodology for this study, as it allows both electron irradiation and detailed nanoscale structural characterization. Also discussed are the types of compounds formed via electronic excitation.

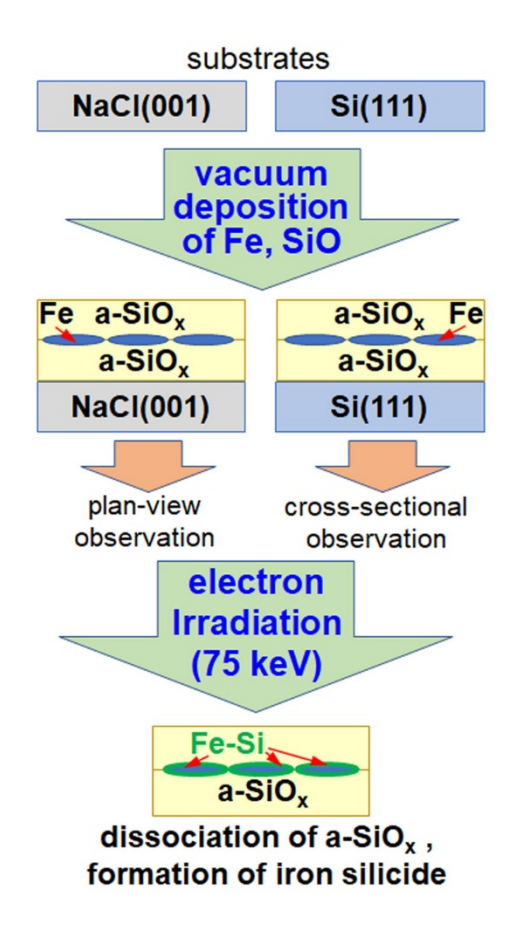
EXPERIMENTAL PROCEDURES

The protocol from sample preparation to electron irradiation is shown in Scheme 1.

Specimen Preparation. Composite thin films of Fe and a-SiO_x (hereafter, a-SiO_x/Fe/a-SiO_x) were prepared by sequential vacuum vapor deposition of silicon monoxide (SiO, 99.99%) and Fe (99.99%) onto NaCl(001) and Si(111) substrates. Each deposition was carried out by heating the above raw material set in a tungsten wire basket at a vacuum of 5×10^{-5} Pa. A quartz thickness monitor attached to the vacuum chamber was used to estimate the average thickness of the deposited layer. The deposited thicknesses for SiO and Fe were set to 8-15 nm and 6-10 nm, respectively (note that these values may differ from the actual film thickness). The oxygen content, x, in the a-SiO_x film was approximately 1.5 as determined by the preceding study³. The substrate temperature was kept at room temperature during the deposition. The as-deposited films prepared on the NaCl substrates were removed by immersing the substrate into distilled water and were mounted onto copper grids for TEM observation (plan-view observation). Cross-sectional TEM specimens were prepared from the films deposited on the Si(111) substrate using a focused ion beam

(FIB) instrument (Thermo Fisher Scientific Scios2 Dual Beam) (cross-sectional view observation).

Electron Irradiation and TEM Observation. The prepared thin films on copper grids (plan-view observation) were irradiated with 75 keV electrons using a TEM (Hitachi H-7000 with a LaB₆ cathode). The electron dose rate was estimated using a Faraday cage attached to the TEM. Dose rate used for the electron irradiation experiments was 1.4×10²⁴ e/m²s. Irradiation was carried out at 298 K and 90 K. A liquid nitrogen-cooled specimen stage equipped with thermocouple was used for low-temperature observations. It is noted that in cross-sectional TEM observation, electron irradiation was carried out in the direction parallel to the Fe/a-SiO_x interface. Structural changes by electron irradiation were observed *in-situ* using the aforementioned 75kV-TEM. High-resolution TEM (HREM) images were observed using a 200 kV-TEM (JEOL JEM-ARM200F with a Schottky field emission gun). TEM images and selected area electron diffraction (SAED) patterns were recorded using a CCD camera (Gatan Orius200 attached to the 75 kV-TEM) or a CMOS camera (Gatan OneView attached to the 200 kV-TEM). Compositional analysis was performed in scanning mode (STEM) using an energy-dispersive x-ray spectrometer (EDS, JEOL JED-2300) attached to the 200 kV-TEM. Specimen thickness was measured by electron energy-loss spectroscopy (EELS) using a post-column energy filter (Gatan ContiniumK3).



Scheme 1. Schematic diagram showing the synthesis process of a-SiO_x/Fe/a-SiO_x composite thin films followed by iron silicide formation induced by electron irradiation.

RESULTS

Electron Irradiation at 298 K and Plan-view TEM observation. Figure 1a and 1b show a bright-field (BF) TEM image and the corresponding SAED pattern of an as-deposited a-SiO_x/Fe/a-SiO_x thin film, respectively. A maze-like contrast is seen on the BF-TEM image. The SAED pattern is composed of Debye-Scherrer rings of body-centered cubic (bcc) Fe and a weak halo ring of a-SiO_x. Thus, a maze-like contrast seen in the BF-TEM image arose from the discontinuous bcc-Fe thin film. No diffraction spots originating from iron oxide were observed. After 75 keV electron irradiation at 298 K for 7.2 ks, the

morphology of the thin film significantly changed as shown in Figure 1c. The total electron dose irradiated was 1.0×10^{28} e/m². Extensive coalescence and growth of Fe nanostructures occurred during electron irradiation. Figure 1d shows the SAED pattern after 75 keV electron irradiation. As can be seen, Debye-Scherrer rings other than bcc-Fe appeared after electron irradiation. These diffraction rings can be indexed by the trigonal Fe₂Si phase (Fe₂Si-type structure, $P\overline{3}m1$)¹³. A schematic diagram of the crystal structure of the trigonal Fe₂Si is shown in Figure S1 in the Supporting Information. Lattice parameters derived from the SAED pattern were a = 0.403(1) nm and c = 0.512(1) nm (the numbers in brackets indicate the standard deviation). These values are almost equivalent to those reported in the literature¹³. It should be noted that under 75 keV-electron irradiation, atomic migration induced by knock-on atom displacement can be excluded since the electron energy of 75 keV is below the threshold of knock-on atom displacement both for Fe (370 kV) and Si (216 kV, or 197 kV for Si in SiO₂)^{14, 15}. Therefore, the formation of Fe₂Si was likely caused by the same mechanism as in the Pt/a-SiO_x system, i.e., the dissociation of a-SiO_x due to electronic excitation⁴. That is, Si-O bonds dissociate through Auger decay of core-holes generated by electronic excitation, and then Fe-Si bonds are formed. The effect of electron irradiation during TEM observation on silicide formation can be negligible because the total dose of electrons during TEM observation ($\sim 10^{24}$ e/m²) is about 10² times lower than that required for silicide formation (>2×10²⁶ e/m²)⁶, and about 10⁴ times lower than that used for the electron irradiation experiments performed in this study (Figure 1).

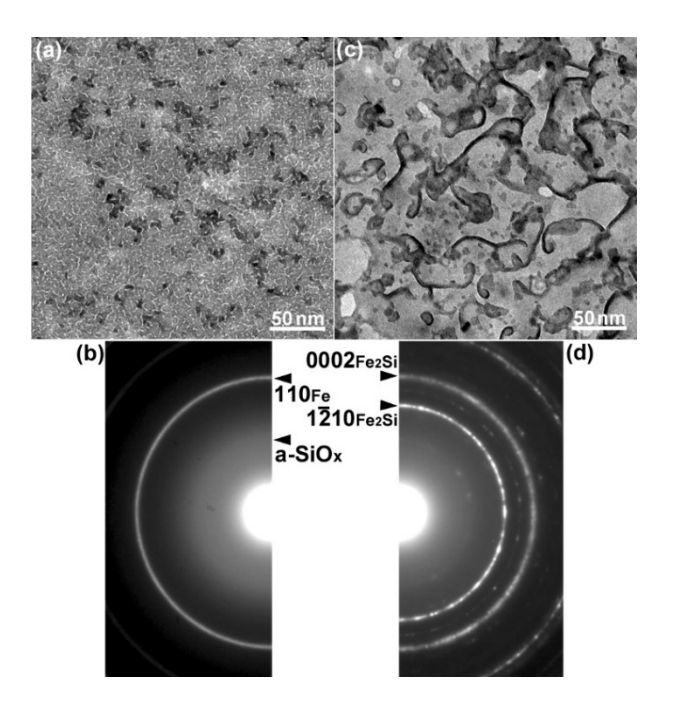


Figure 1. BF-TEM images and SAED patterns of an a-SiO_x/Fe/a-SiO_x thin film. (a, b) as-deposited, (c, d) after 75 keV electron irradiation at 298 K for 7.2 ks (total dose: 1.0×10^{28} e/m²).

Figure 2a shows the intensity profiles of the SAED patterns obtained for the as-deposited and the irradiated specimens shown in Figure 1. The intensity was integrated in the circumferential direction. As-deposited specimen was composed of bcc-Fe and a-SiO_x. Intensity profiles clearly shows the formation of Fe₂Si upon electron irradiation. Note that the Miller-Bravais indices of hkil represent the trigonal structure (Fe₂Si). No diffraction peaks due to Fe oxides were observed. This can be attributed to the fact that as the Si-O bonds in a-SiO_x dissociate and Si-metal bonds form, the matrix composition approaches SiO₂, as demonstrated in our previous study⁴. This result shows the robustness of the methodology; a silicide formation is possible for elements that have a lower affinity for oxygen than Si. Figure 2b shows a magnified SAED pattern after electron irradiation. Weak spots of 200_{Fe} remains as indicated by an arrow, which is difficult to discern in the intensity profile because it overlaps with the tail of the $02\overline{2}2Fe_2Si$. Thus,

it was found that trigonal Fe₂Si was formed when irradiated with 75 keV electrons at 298 K, while a small amount of unreacted bcc-Fe remained.

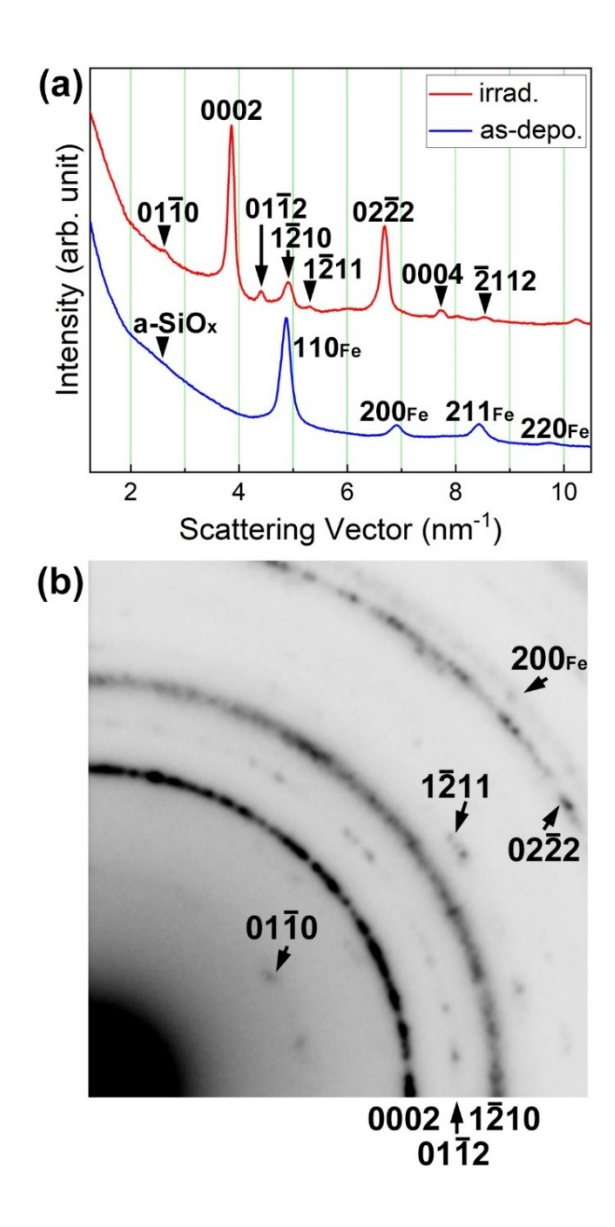


Figure 2. (a) Intensity profiles of the SAED patterns obtained for the as-deposited and the irradiated specimens shown in Figure 1. (b) A magnified SAED pattern after electron irradiation.

Figure 3a shows an HREM image observed in the irradiated area of the specimen shown in Figure 1c. The upper left inset shows the entire area where significant coalescence and growth occurred by electron irradiation. The HREM image shows distribution of (0002) lattice fringes of the trigonal Fe₂Si with lattice spacing of 0.25 nm. The size of the region containing Fe₂Si is approximately 10 nm in diameter, and each grain oriented in different directions. This corresponds to a continuous Debye-Scherrer rings shown in Figure 1d. Thus, formation of the Fe₂Si in a local region was confirmed. Figure 3b shows a magnified HREM image of the area indicated by an arrowhead in Figure 3a, including the interface between Fe₂Si and a-SiO_x. Clear (0002) lattice fringes are observed in the Fe₂Si region. The interface between the crystalline and amorphous phases is indicated by a dotted line. As seen, the interface is not flat, but has a complex shape. No compounds such as Fe oxides other than Fe₂Si or a-SiO_x are observed at the interface.

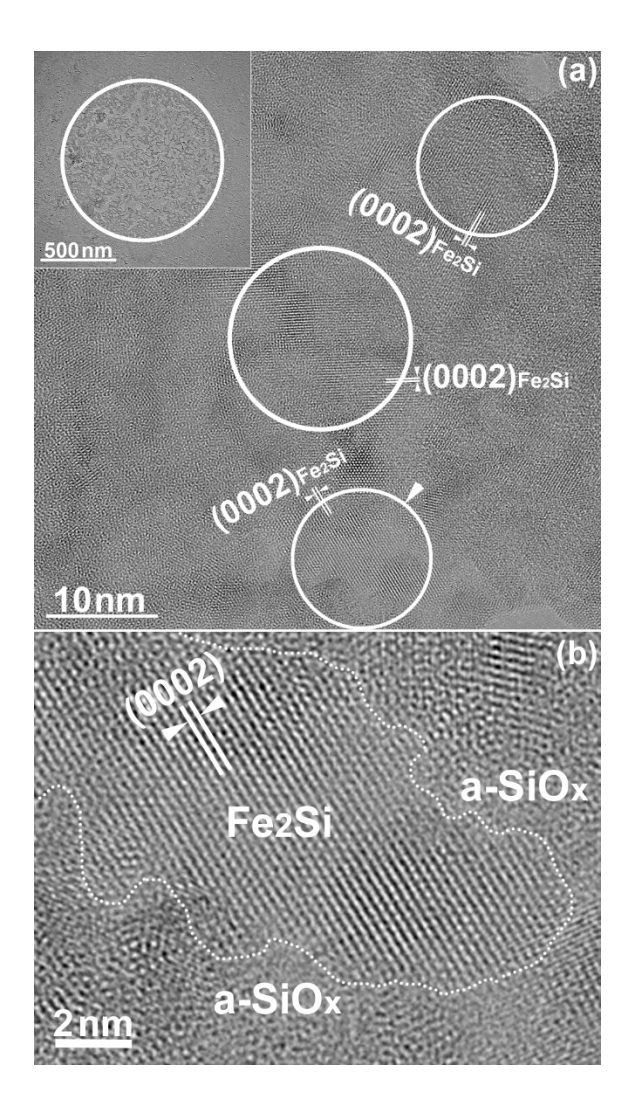


Figure 3. (a) HREM image observed in the irradiated area of the specimen shown in Figure 1c. The upper left inset indicates the area where significant morphological change occurred. (b) A magnified HREM image of the area indicated by an arrowhead in Figure 3a, including the interface between Fe₂Si and a-SiO_x.

Figure 4 shows the results of STEM-EDS elemental mapping of the irradiated area of the specimen shown in Figure 1c. Distribution of Fe, Si, and O are displayed with green, red, and blue, respectively. The elemental map clearly shows that green region surrounds purple region; namely, Fe-rich region (Fe₂Si

or bcc-Fe) surrounds a-SiO_x. This is the result of remarkable grain growth occurring in the Fe thin film with the formation of Fe₂Si; it is inferred that significant migration of Fe and Si occurs in search of a new Fe/Si interface. Similar tendency was also observed in the Pt/a-SiO_x system after electron irradiation⁶.

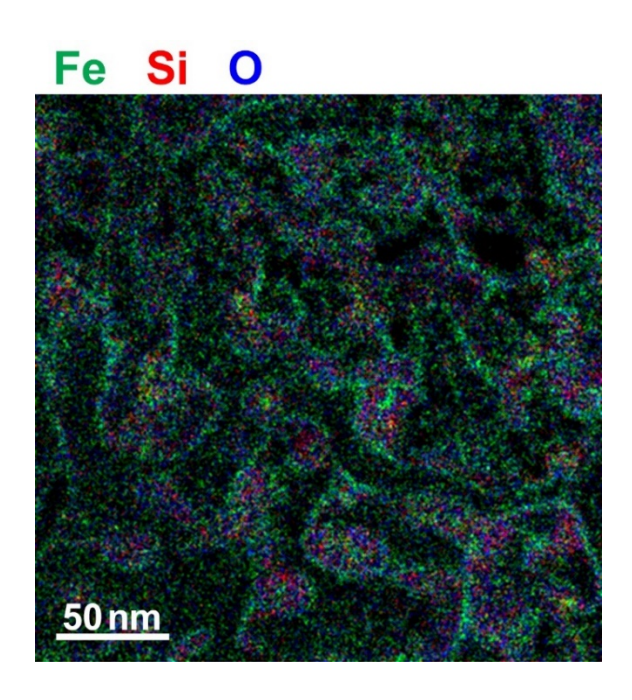


Figure 4. STEM-EDS elemental map of the irradiated area. Distribution of Fe, Si, and O are displayed with green, red, and blue, respectively.

Electron Irradiation at 90 K and Plan-view TEM Observation. Figure 5a and 5b show a BF-TEM image and the corresponding SAED pattern of an as-deposited a-SiO_x/Fe/a-SiO_x thin film, respectively, observed at 90 K. A maze-like contrast is seen on the BF-TEM image. The SAED pattern is composed of Debye-Scherrer rings of bcc-Fe and a weak halo ring of a-SiO_x. No diffraction spots originating from iron oxide were observed. There is no change in the thin film structure of the as-deposited specimen compared to that observed at 298 K (Figure 1a). Figure 5c and 5d show a BF-TEM image and the corresponding

SAED pattern after 75 keV electron irradiation at 90 K for 7.2 ks. The total electron dose irradiated was 1.0×10^{28} e/m² (same conditions as irradiation experiment performed at 298 K). As shown in the SAED pattern, trigonal Fe₂Si was formed at 90 K, but no significant grain growth was observed in the thin film structure. Some of the reflections such as $01\overline{10}$, $01\overline{12}$, and $1\overline{2}11$, which were weak in intensity even at 298 K (see Figure 2b), are not visible in Figure 5d. This fact may suggest that the migration rates of Fe and Si for the Fe₂Si formation depend on temperature. This can be understood from the fact that the solid-state reaction between Fe and Si requires high temperatures of around 1000 K ⁷⁻¹⁰. It can be concluded that Fe₂Si formation is realized by 75 keV irradiation at 90 K at a somewhat reduced rate as compared to the irradiation at 298 K.

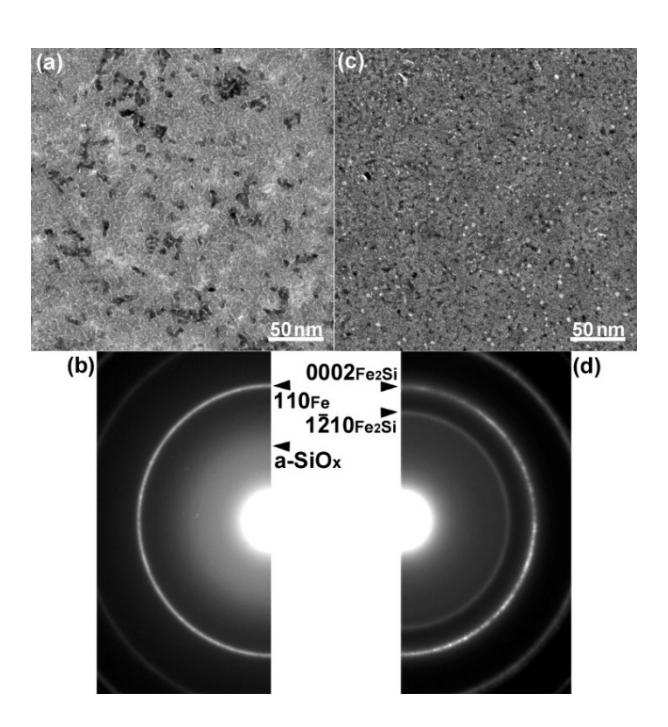


Figure 5. BF-TEM images and SAED patterns of an a-SiO_x/Fe/a-SiO_x thin film. (a, b) as-deposited, (c, d) after 75 keV electron irradiation at 90 K for 7.2 ks (total dose: 1.0×10^{28} e/m²).

Cross-sectional TEM observation. Figure 6a shows the STEM-EDS elemental map obtained for a cross-sectional specimen after 75 keV electron irradiation at 298 K. Distribution of Fe (green), Si (red), O (blue) are evident. The total electron dose irradiated was 1.0×10²⁸ e/m² at 75 keV. As the elemental map shows, the Fe-rich layer (Fe₂Si nanosheets) maintains its layered structure even after electron irradiation. This tendency is consistent with our previous studies on the Pt/a-SiO_x system⁶. Thus, it is plausible that the grain growth observed in Figure 1c occurred mainly in the lateral direction of the thin film. Figure 6b shows concentration profiles extracted from the STEM-EDS elemental map shown in Figure 6a. The origin of the distance was assigned to the Si/a-SiO_x interface, and the scale on the vertical axis is the same in Figure 6a and 6b. Concentration was quantified based on the thin film approximation assuming the theoretical k-factor¹⁶. For this reason, the derived concentration of light elements, especially oxygen, is not quantitative. The trace amount of oxygen in the Si substrate region is due to the thin surface oxide layer on the cross-sectional TEM specimen. A small bump in Fe concentration near the distance of 15 nm is presumed to be an artifact due to redeposition during FIB-microsampling. A noteworthy point is that the Si concentration increases significantly at the Fe/a-SiO_x interfaces as indicated by arrows. The increase in Si concentration is remarkable compared with the previous experimental results for the Pt/a-SiO_x system⁶. This is because the electron flux used in this study was 20 times higher than that used in the previous study⁶, and hence the dissociation of a-SiO_x could have been enhanced. The local increase in Si concentration in electron-irradiated a-SiO_x is direct evidence for the dissociation of a-SiO_x.

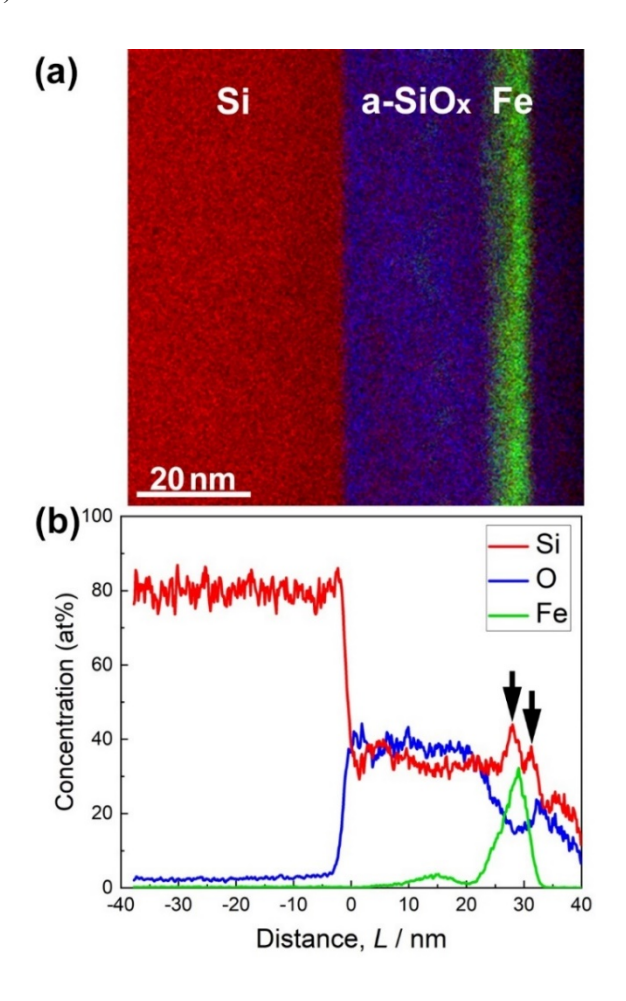


Figure 6. (a) STEM-EDS elemental map of the cross-section of a-SiO_x/Fe/a-SiO_x/Si(111) after 75 keV electron irradiation at 298 K for 7.2 ks (total dose: 1.0×10^{28} e/m²). (b) Composition profiles extracted from the STEM-EDS map.

DISCUSSION

As mentioned in the experimental section, trigonal Fe₂Si was formed at the Fe/a-SiO_x interface by electron irradiation. Figure 7 shows a schematic illustration showing the elementary processes of the interfacial reaction proposed in this study, including previous findings^{4, 17}; (1) electronic excitation of a-SiO_x (x~1.5) (Si³⁺ \rightarrow Si⁴⁺) by electron irradiation, (2) Auger decay of a core-hole, (3) dissociation of a Si-

O bond, and (4) formation of an Fe-Si bond. The dissociation mechanism triggered by electronic excitation is similar to the case in the Knotek-Feibelman (K-F) model for oxygen ion desorption from the free surface of oxides². Note that the illustration shown in Figure 7 exaggerates the desorption of oxygen since such desorption of oxygen does not occur except at the surface. Instead, recombination of Si-O bonds occurs, or it is also possible for Si atoms that become free from O atoms for a short time can be trapped by Fe atoms at the Fe/a-SiO_x interface. All these processes occur repeatedly during electron irradiation. In this manner, it is possible to form Fe₂Si at the Fe/a-SiO_x interface.

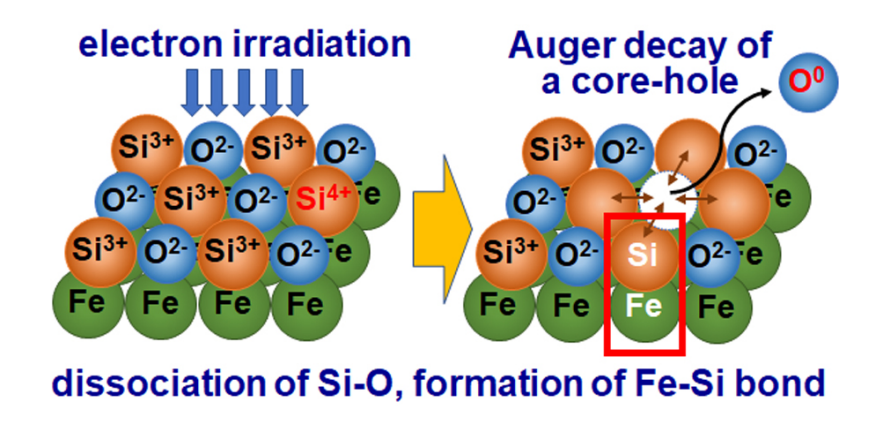


Figure 7. Schematic illustration showing the elementary processes of the novel interfacial reaction proposed in this study; dissociation of a Si-O bond, and formation of an Fe-Si bond.

Walser and Bené proposed a rule for the first compound formed at the planar interface between transition metal and Si¹⁸. According to their study, equiatomic FeSi was the predicted compound and in fact observed between Fe and Si. Similarly, the effective heat of formation (EHF) model proposed by Pretorius et al. predicts the formation of the FeSi as the first phase formed between Fe and Si¹⁹. The results of this study appear to contradict these thermodynamical predictions, but this is thought to be due to the difference between compound formation at a planar interface by ordinally thermal annealing and solid-

state reaction due to electronic excitation. In the present study, it is atomic Si rather than planar Si that forms the interface with Fe, and the above model may not be directly applicable.

To explore the possibility of the formation of other types of compounds besides Fe₂Si, we attempted long-term electron irradiation up to 28.8 ks (total dose: 4.0×10^{28} e/m²), but no Fe-Si compounds other than Fe₂Si were formed. Figure S2 in the Supporting Information shows the intensity profiles of the SAED patterns obtained for the specimens with different irradiation times. As the electron irradiation proceeded, intensity of 0002Fe₂Si reflection increased, and the peak position of 110Fe and/or $1\overline{2}10$ Fe₂Si reflection shifted slightly towards higher scattering angles. Since the 110Fe reflection almost overlaps with the $1\overline{2}10$ Fe₂Si, above mentioned change indicates Fe consumption associated with the Fe₂Si formation. Under the irradiation conditions used in this study, no signs of the formation of Fe-Si compounds other than Fe₂Si were observed. This means that Si concentration did not increase more than ~33at% (Fe₂Si) during the prolonged electron irradiation up to 28.8 ks. The factors that stabilize Fe₂Si remain unresolved.

We also examined the effect of oxygen content on the silicide formation; namely, a similar irradiation experiments were conducted using a-SiO₂ instead of a-SiO_x ($x\sim1.5$). a-SiO₂/Fe/a-SiO₂ thin films were fabricated by RF magnetron sputtering as described in the Supporting Information. Figure S3 in the Supporting Information compares the SAED patterns obtained for a-SiO_x/Fe/a-SiO_x (Figure S3a) and a-SiO₂/Fe/a-SiO₂ (Figure S3b) thin films after 75 keV electron irradiation at 298 K (total dose: 1.0×10^{28} e/m²). As seen, Fe₂Si was also formed in the a-SiO₂/Fe/a-SiO₂ thin film, while some of the reflections such as $01\overline{1}0$ and $01\overline{1}2$ are not visible. This indicates that Fe₂Si formation is slower at the Fe/a-SiO₂ interface than that at the Fe/a-SiO_x. This is presumably because a-SiO₂ is chemically more stable than a-SiO_x($x\sim1.5$), and Si-O bonds are less likely to dissociate due to electronic excitation. Chen et al.²⁰ reported the formation of Si nanostructures in a-SiO₂ thin film by 100 keV-electron irradiation with a high electron dose (3×10^{28} e/m²) similar to the present study ($1-4\times10^{28}$ e/m²), while they used electron flux of $\sim7.5\times10^{27}$

e/m²s, which was three orders of magnitude higher than that used in this study $(1.4\times10^{24} \text{ e/m}^2\text{s})$. They stated that a-SiO₂ is very insensitive to electron-beam irradiation, requiring a threshold dose as high as 10^{28} e/m^2 to transform completely into silicon. In contrast, the threshold electron dose for solid-state reactions in the metal/a-SiO_x system due to electron irradiation is $2\times10^{26} \text{ e/m}^2$ (ref.6). Thus, based on previous findings and the results obtained in this study, it is evident that a-SiO_x is more easily dissociated by electron irradiation compared to a-SiO₂.

Regarding the temperature dependence of the interfacial reaction due to electronic excitation, the reaction was more accelerated at room temperature (comparison of Figure 1d (298 K) and Figure 5d (90 K)), suggesting that the atomic migration depends on temperature in a natural manner. A possible temperature rise during electron irradiation was estimated using the method reported by Jenčič et al.²¹ The obtained value was about 2 K and is therefore practically negligible. Similar temperature dependence was observed in the electron irradiation induced crystallization of a Pd-Si amorphous thin film embedded in a-SiO_x thin films²², but no clear temperature dependence was observed in Pt₂Si formation at the Pt/SiO_x interface (significant reaction occurred even at 90 K)⁶. Reactivity of metal element with Si may be involved in the aforementioned temperature dependence of the solid-state reaction. Further study is needed on this point.

Interfacial reaction similar to this study was reported for Pd/Al₂O₃ system; reduction of Al₂O₃ was induced by 300 keV electron irradiation which eventually led to the formation of metastable Al₂Pd ²³. Thus, dissociation of oxides by electronic excitation is a highly versatile method for producing metal-metalloid or intermetallic compounds at room temperature. Electronic excitation also induces crystallization of amorphous Ge thin films, which was recently demonstrated by using low-energy electrons (2-20 keV)²⁴. A plasma bombing strategy has been demonstrated as a method for synthesizing materials via excitation²⁵. These reports suggest that electronic excitation may be useful for creation and

modification of novel materials.

CONCLUSIONS

We studied the nanoscale solid-state reaction at the Fe/a-SiO_x thin film interface using electron irradiation. Trigonal Fe₂Si nanosheets were formed by 75 keV electron irradiation at 90 K as well as at 298 K. Low temperature synthesis of the Fe₂Si can be attributed to the dissociation of a-SiO_x induced by electronic excitation, since the 75 keV electron irradiation is below the threshold of knock-on atom displacement both for Fe and Si. In the process, Si-O bonds dissociate through Auger decay of core-holes generated by electronic excitation, and then Fe-Si bonds are formed. The degree of solid-state reaction was more significant at 298 K, suggesting that atomic migration induced by electronic excitation involves contribution of thermal energy. Experimental results suggest that the Si-O bond dissociates more easily in a-SiO_x than in a-SiO₂ by electronic excitation. Formation of the Fe₂Si induced by electronic excitation differs from the equiatomic FeSi formation at an Fe/Si planar interface via thermal annealing. By using the method proposed in this study, it is possible to form metal silicide nanosheets site-selectively in an electron irradiated area at temperatures below room temperature. Future prospect includes the enhancement of volume fraction of Fe₂Si by, for example, periodically arranging the electron irradiation areas, making it possible to measure magnetic properties of the Fe₂Si nanosheets and contribute to the synthesis of spintronics nanodevices.

ASSOCIATED CONTENT

Supporting Information

The Supporting Information is available free of charge at

Crystal structure, intensity profiles after prolonged irradiation, results on a-SiO₂/Fe/a-SiO₂ thin films

AUTHOR INFORMATION

Corresponding Author

Kazuhisa Sato –Research Center for Ultra-High Voltage Electron Microscopy, Osaka University, 7-1 Mihogaoka, Ibaraki, Osaka 567-0047, Japan; orcid.org/0000-0001-9078-2541; E-mail: sato@uhvem.osaka-u.ac.jp

Author

Yuta Fujii –Research Center for Ultra-High Voltage Electron Microscopy, Osaka University, 7-1 Mihogaoka, Ibaraki, Osaka 567-0047, Japan

Author Contributions

Kazuhisa Sato: Conceptualization, Investigation, Methodology, Formal Analysis, Funding Acquisition, Supervision, Writing-original draft. **Yuta Fujii**: Investigation, Formal Analysis

Notes

The authors declare no conflict of interest.

ACKNOWLEDGMENTS

This study was partially supported by the JSPS KAKENHI (Grant No. 24K01159 and No.21H01764). The authors wish to thank Mr. T. Yasuda and Dr. S. Takagi of Osaka University for their helps in this study.

REFERENCES

- (1) Defects and Defect Processes in Nonmetallic Solids; Hayes, W.; Stoneham, A. M.; Dover Publications Inc: Mineloa, New York, 1985.
- (2) Knotek, M. L.; Feibelman, P. J. Ion-desorption by core-hole Auger decay. *Phys. Rev. Lett.* **1978**, *40*, 964–967.
- (3) Lee, J. -G.; Nagase, T.; Yasuda, H.; Mori, H. Synthesis of metal silicide at metal/silicon oxide interface by electronic excitation. *J. Appl. Phys.* **2015**, *117*, 194307.
- (4) Sato, K.; Yasuda, H.; Ichikawa, S.; Imamura, M.; Takahashi, K.; Hata, S.; Matsumura, S.; Anada, S.; Lee, J.-G.; Mori, H. Synthesis of platinum silicide at platinum/silicon oxide interface by photon irradiation. *Acta Mater.* **2018**, *154*, 284–294.
- (5) Ono, L. K.; Croy, J. R.; Heinrich, H.; Cuenya, B. R. Oxygen chemisorption, formation, and thermal stability of Pt oxides on Pt nanoparticles supported on SiO₂/Si(001): size effects. *J. Phys. Chem. C* **2011**, *115*, 16856–16866.
- (6) Sato, K.; Mori, H. Athermal solid phase reaction in Pt/SiO_x thin films induced by electron irradiation. *ACS Omega* **2021**, *6*, 21837–21841.
- (7) Binary Alloy Phase Diagrams; Massalski, T. B.; Murray, J. L.; Bennett, L. H.; Kacprzak, L., Eds.; ASM: Metals Park, OH, 1986.
- (8) Leong, D.; Harry, M.; Reeson, K. J.; Homewood, K. P. A silicon/iron-disilicide light-emitting diode operating at a wave length of 1.5μm. *Nature* **1997**, *387*, 686–688.
- (9) Suemasu, T.; Negishi, Y.; Takakura, K.; Hasegawa, F.; Chikyow, T. Influence of Si growth temperature for embedding β-FeSi₂ and resultant strain in β-FeSi₂ on light emission from p-Si/β-FeSi₂ particles/n-Si light-emitting diodes. *Appl. Phys. Lett.* **2001**, *79*, 1804–1806.
- (10) Won, J. H.; Sato, K.; Ishimaru, M.; Hirotsu, Y. Transmission electron microscopy study on FeSi₂

- ACS Appl. Nano Mater. 7 (2024) 16799-16805.
- nanoparticles synthesized by electron-beam evaporation. J. Appl. Phys. 2006, 100, 014307.
- (11) Tang, C. P.; Tam, K. V.; Xiong, S. J.; Cao, J.; Zhang, X. The structure and electronic properties of hexagonal Fe₂Si. *AIP adv.* **2016**, *6*, 065317.
- (12) Sun, Y.; Zhuo, Z.; Wu, X.; Yang, J. Room temperature ferromagnetism in two-dimensional Fe₂Si nanosheet with enhanced spin-polarized ratio. *Nano Lett.* **2017**, *17*, 2771–2777.
- (13) Pearson's Handbook Desk Edition. Villars, P.; ASM International: Materials Park, OH, 1997.
- (14) Urban, K. Radiation-induced processes in experiments carried out in-situ in the high-voltage electron microscope. *Phys. Stat. Sol. (a)* **1979**, *56*, 157–168.
- (15) Pfeffer, R. L. Damage center formation in SiO₂ thin films by fast electron irradiation. *J. Appl. Phys.* **1985**, *57*, 5176–5180.
- (16) Cliff, G.; Lorimer, G. W. The quantitative analysis of thin specimens. *J. Microsc.* **1975**, *103*, 203–207.
- (17) Yasuda, H.; Sato, K.; Ichikawa, S.; Imamura, M.; Takahashi, K.; Mori, H. Promotion in solid phase reaction of Pt/SiO_x bilayer film by electron-orbital-selective-excitation. RSC Adv. **2021**, *11*, 894–898.
- (18) Walser, R. M.; Bené, R. W. First phase nucleation in silicon-transition-metal planar interfaces. *Appl. Phys. Lett.* **1976**, *28*, 624–625.
- (19) Pretorius, R.; Marais, T. K.; Theron, C. C. Thin film compound phase formation sequence: An effective heat of formation model. *Mat. Sci. Eng.* **1993**, *10*, 1–83.
- (20) Chen, G. S.; Boothroyd, C. B.; Humphreys, C. J. Electron-beam-induced damage in amorphous SiO₂ and the direct fabrication of silicon nanostructures. *Phil. Mag. A* **1998**, *78*, 491–506.
- (21) Jenčič, I.; Bench, M. W.; Robertson, I. M.; Kirk, M. A. Electron-beam-induced crystallization of isolated amorphous regions in Si, Ge, GaP, and GaAs. *J. Appl. Phys.* **1995**, *78*, 974–982.
- (22) Sato, K.; Mori, H. Solute atom mediated crystallization of amorphous alloys. Materialia 2023, 32,

101888.

- (23) Kamino, T.; Kuroda, K.; Saka, H. In situ HREM/microanalysis study of reduction of Al₂O₃ with palladium. *Ultramicrosc.* **1992**, *41*, 245–248.
- (24) Nakamura, R.; Matsumoto, A.; Ishimaru, M. Explosive crystallization of sputter-deposited amorphous germanium films by irradiation with an electron beam of SEM-level energies. *J. App. Phys.* **2021**, *129*, 215301.
- (25) Rao, P.; Wu, D.; Luo, J.; Li, J.; Deng, P.; Shen, Y.; Tian, X. A plasma bombing strategy to synthesize high-loading single-atom catalysts for oxygen reduction reaction. *Cell Reports Phys. Sci.* **2022**, *3*, 100880.